Epitaxial Fe/Cu superlattices on Si(111)

W. H. Schreiner, D. H. Mosca, S. R. Teixeira, and N. Mattoso

Citation: Journal of Applied Physics **72**, 5682 (1992); doi: 10.1063/1.351918
View online: http://dx.doi.org/10.1063/1.351918
View Table of Contents: http://scitation.aip.org/content/aip/journal/jap/72/12?ver=pdfcov
Published by the AIP Publishing

Epitaxial Fe/Cu superlattices on Si(111)

W. H. Schreiner, D. H. Mosca, and S. R. Teixeira
Laboratório de Filmes Finos, Instituto de Fisica da UFRGS, Caixa Postal 15051, 91501-970 Porto Alegre, RS, Brazil

N. Mattoso
Laboratório de Estudos de Materiais e Interfaces-COPPE UFRJ, Caixa Postal 68505, 21945 Rio de Janeiro, RJ, Brazil

(Received 22 January 1992; accepted for publication 30 August 1992)

We report on the successful epitaxial growth of Fe/Cu superlattices on Si(111) wafers at room temperature. The superlattices were characterized with x-ray diffraction, conversion electron Mössbauer spectrometry, and selected area electron diffraction experiments. The epitaxial growth is crucially dependent on which element is deposited first on the bare Si(111).

INTRODUCTION

Recently Cheng *et al.*[1] have shown that epitaxial bcc Fe films up to several thousand Angströms could be grown on Si(111) substrates at room temperature (RT). These films displayed the Fe(111) orientation normal to the substrate surface and an alignment of the (110) direction of Fe and Si within the substrate plane.

Copper is relatively easier to grow and fairly thick films despite an appreciable lattice mismatch grow epitaxially on Si(100) and Si(111) according to Chang[2] at RT.

The question is if it is possible to grow epitaxial superlattices of Fe/Cu on Si(111) directly. There is a wealth of information in the literature on epitaxial growth of Fe on Cu and vice-versa.[3–18] Jesser and Matthews[3] were the first to report on the growth of fcc Fe on Cu(100) substrates. Gradmann and Tillmans[4] found layer by layer growth of fcc Fe on Cu(111) for films up to 8 Å at RT. For thicker films the Fe gradually goes over the bcc crystalline form. There followed a big controversy[5–8] if these epitaxial Fe films were para-, ferro-, or antiferromagnetic at RT. Freeman and Fu[9] contributed to this topic from the theoretical standpoint showing that fcc Fe can display different magnetic ordering depending on it crystalline lattice parameter. Heinrich *et al.*[10] grew bcc Cu(100) on bcc Fe(100) and have shown that Cu could be grown in a bcc structure up to 10 monolayers before undergoing a transition to fcc Cu for thicker films. They also showed that epitaxial bcc Fe(100) can be grown on top of bcc Cu(100). In epitaxial Fe/Cu/Fe trilayers Celinsky and Heinrich[11] found antiferromagnetic coupling between Fe layers for certain Cu layer thicknesses.

Pontkees and Neddermeyer[12] produced low monolayer epitaxial Cu/Fe/Cu(111) sandwiches. Bennett *et al.*[13] found an oscillatory behavior of the interlayer exchange using the Kerr effect in fcc Fe(100)/Cu/fcc Fe(100) sandwiches grown on Cu(100). Experiments on Fe/Cu multilayers confirmed that this is a new system with an oscillatory interlayer coupling. Parkin *et al.*[15] grew Fe/Cu multilayers by sputtering on Si(100) and Si(111) and found this oscillatory effect for polycrystalline films. Petroff *et al.*[16] reported on oscillatory interlayer exchange and on a large magnetoresistance of the spin-valve type in Fe/Cu multilayers grown on Si(100) substrates. They find highly textured multilayers with clear bcc Fe and mixed bcc and fcc Cu layers depending on the Cu layer thickness.

Thus, the epitaxy of these three elements two by two is fairly well understood and described. This work now addresses the possibility of growing epitaxial Fe/Cu superlattices on Si(111). This topic is important both for fundamental studies of thin film growth of two metals on a semiconductor as well as for applications of these superlattices in magnetic and electronic devices directly integrated on silicon. From a magnetic exchange interaction point of view one could also ask for comparisons between Fe/Cu multilayers with different crystalline orientations, which could greatly advance the understanding of the metallic magnetic multilayers.

SAMPLE PREPARATION

The thin film samples were deposited on bare HF-etched Si(111) wafers at RT in a BALZERS UMS 500P ultravacuum system. The base pressure before deposition was 2×10^{-8} mbar. The evaporation of Fe(4 N) and Cu(6 N) was done with two quartz crystal controlled *e* beams. The deposition rate was 0.5 Å/s for both metals.

Two samples were deposited with the following characteristics: sample 1 a multilayer Si(111)/Fe 15 Å/Cu 15 Å)×10; and sample 2 a multilayer Si(111)/(Cu 15 Å/Fe 15 Å)×10 with a final Cu 15 Å capping layer.

All samples showed a shiny metallic lustre. No special storage precautions were employed and the air exposed samples did not lose their fine finish.

X-RAY DIFFRACTION

The x-ray diffraction was performed on a Siemens machine in the θ-2θ Debye–Scherrer geometry, employing Cu K_α radiation. The low angle results of the two multilayers are shown in Fig. 1. We note the sharp Kiessig[19] fringes which indicate a high quality multilayer.[20] The Bragg peaks associated with the chemical unit cell of the multilayer are not very evident or are buried within the Kiessig fringes. This lack has to be associated with the low contrast of the atomic scattering powers of the Fe and Cu atoms. We find only one Bragg peak for sample 2 at $2\theta=2.88°$.

 0021-8979/92/245682-05$04.00

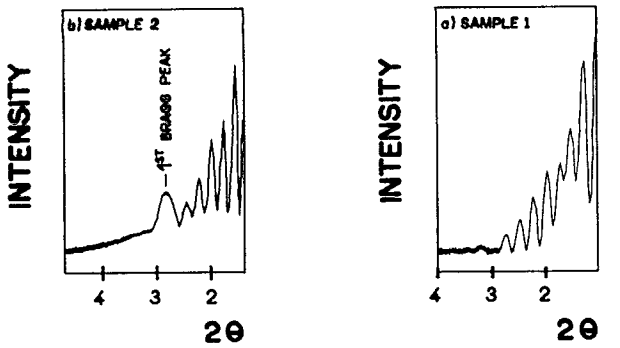

FIG. 1. Low angle x-ray diffractograms of the Fe/Cu multilayers. Note the sharp Kiessig fringes for both samples. Sample 2 displays also a lonely Bragg peak which leads to a calculated modulation length of 31 Å.

Using Bragg's law we find $d=31$ Å for this Cu/Fe bilayer thickness, which is very near to the designed modulation length.

The high angle diffraction results of the samples are shown in Fig. 2. Besides the strong Si(111) and higher order diffraction maxima the two multilayers show only one peak at $2\theta=44.8°$ for sample 1 and $2\theta=137.2°$ for sample 2, respectively. The diffraction peak at $2\theta=137.2°$ can be readily associated with bcc Fe(222) planes lying within the plane of the substrate.[21] The lower angle peak at $2\theta=44.8°$ for sample 1 is not easily interpreted. It can be due to the bcc Fe(110) or to the fcc Cu(111) diffraction.

The high angle diffraction results thus show that both samples are completely textured and that this texture is crucially linked to the metal which is first deposited on Si(111). The bcc Fe(222) line in bulk samples is seventeen times weaker than the Fe(110) line and only highly oriented samples could produce a diffractogram with only one line at the Fe(222) angular position. The θ-2θ Debye–Scherrer geometry is unable to inform us what the crystalline situation is of the samples in other directions different from the normal of the substrate plane. Electron diffraction can help in this aspect as we will show later.

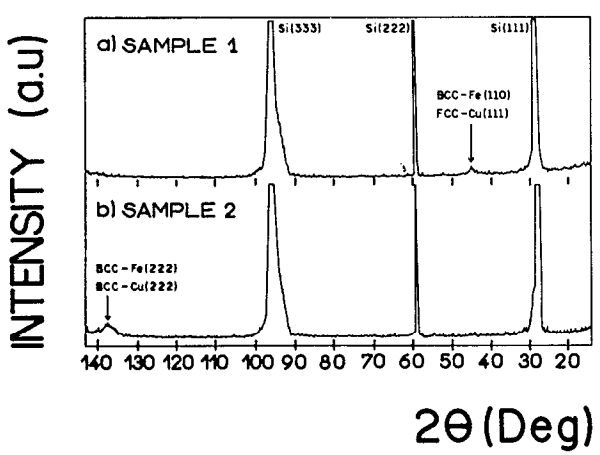

FIG. 2. High angle x-ray diffraction results for the Fe/Cu multilayers on Si(111).

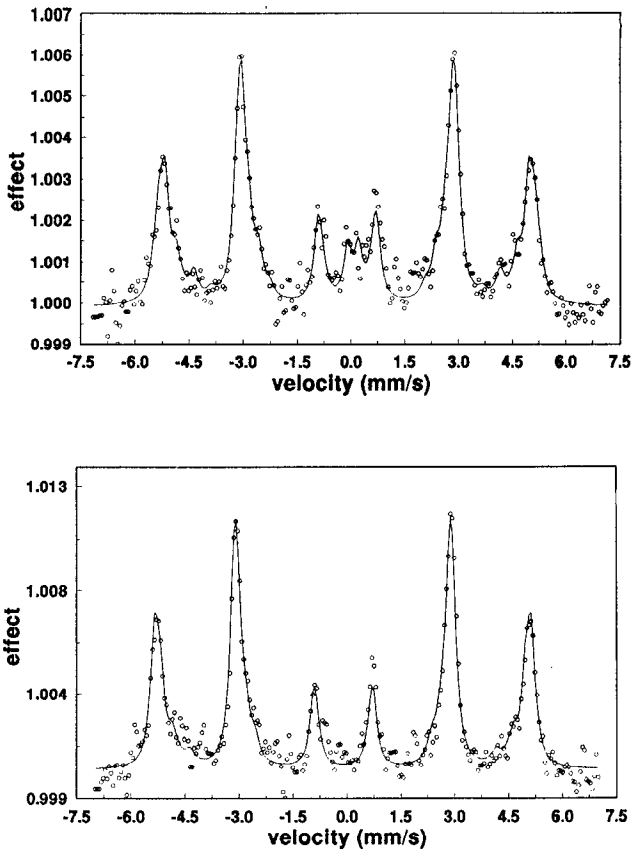

FIG. 3. Conversion electron Mössbauer spectra for the Fe/Cu superlattices: (a) Sample 1 starts with Fe on the bare Si. (b) Sample 2 starts with Cu on Si.

CONVERSION ELECTRON MÖSSBAUER SPECTROSCOPY

The CEMS (conversion electron Mössbauer spectroscopy) spectra were taken in a standard gas flow constant acceleration spectrometer where 7.3 keV conversion electrons resulting from recoilless ^{57}Fe nuclei were detected in a backscattering geometry. We used a ^{57}Co source in a Rh matrix and the fitting parameters are quoted in reference to this source. Figures 3(a) and 3(b) show the CEMS spectra of both Fe/Cu multilayers. Sample 1, which starts with Fe adjacent to Si(111) displays a spectrum with basically a sextet together with a central doublet. The sextet is fairly broad and could be fitted with a distribution of hyperfine fields as shown in Fig. 4(a). The fitting parameters were: isomer shift (IS) $=-0.11$ mm/s and linewidth $\Gamma=0.27$ mm/s. Noteworthy is the broad distribution and the fact that the most probable field is at 315 kOe and not at 330 kOe as should be expected for bcc Fe. The central paramagnetic doublet is not very well resolved and probably comes from the Fe atoms located at the Fe/Cu interfaces. The fitting parameters for this doublet were: quadrupole splitting $\Delta E_Q=0.3$ mm/s, IS $=0.05$ mm/s, and $\Gamma=0.27$ mm/s. Sample 2, which starts with Cu on Si(111) displays a sextet with a much sharper distribution of hyperfine fields. In Fig. 4(b) we show the distribution of hyperfine fields used to fit this spectrum. Also here the hyperfine fields are lower than the expected 330 kOe for bcc Fe and

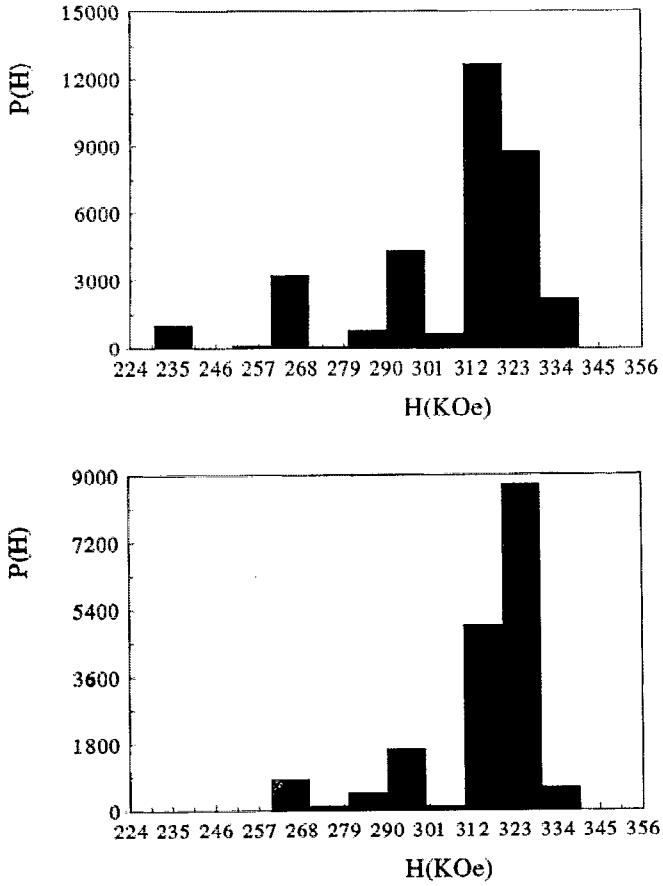

FIG. 4. Distribution of the hyperfine fields obtained by the histogram method used to fit the ferromagnetic sextet of (a) sample 1 and (b) sample 2.

the most probable field is found at 325 kOe. The fitting parameters were: IS $=-0.11$ mm/s and $\Gamma=0.27$ mm/s. The central structure observed for sample 1 is absent here.

ELECTRON DIFFRACTION

The electron diffraction experiments were performed on a JEOL JEM 2000FX transmission electron microscope operating at 200 kV and a current of 125 μA. The silicon at the back of the samples was etched chemically from the backside with a HF-HNO_3 mixture to admit transmission of the electrons. The electrons had an incidence perpendicular to the Si substrate. Figure 5(a) shows the electron diffraction pattern of a selected area of the Fe/Cu multilayer which starts with Fe on top of Si(111). Besides the hexagonal Si pattern we see clearly the diffraction spots due to Fe and Cu as well as "decorated" Si diffraction spots. Figure 5(b) shows the diffraction pattern of the second multilayer which starts with Cu on top of Si(111). The monocrystallinity of the multilayer components also appears here. Very interesting, however, is the different orientation of Fe and Cu relative to the silicon substrate. The satellites now appear angularly displaced relative to the Si spots.

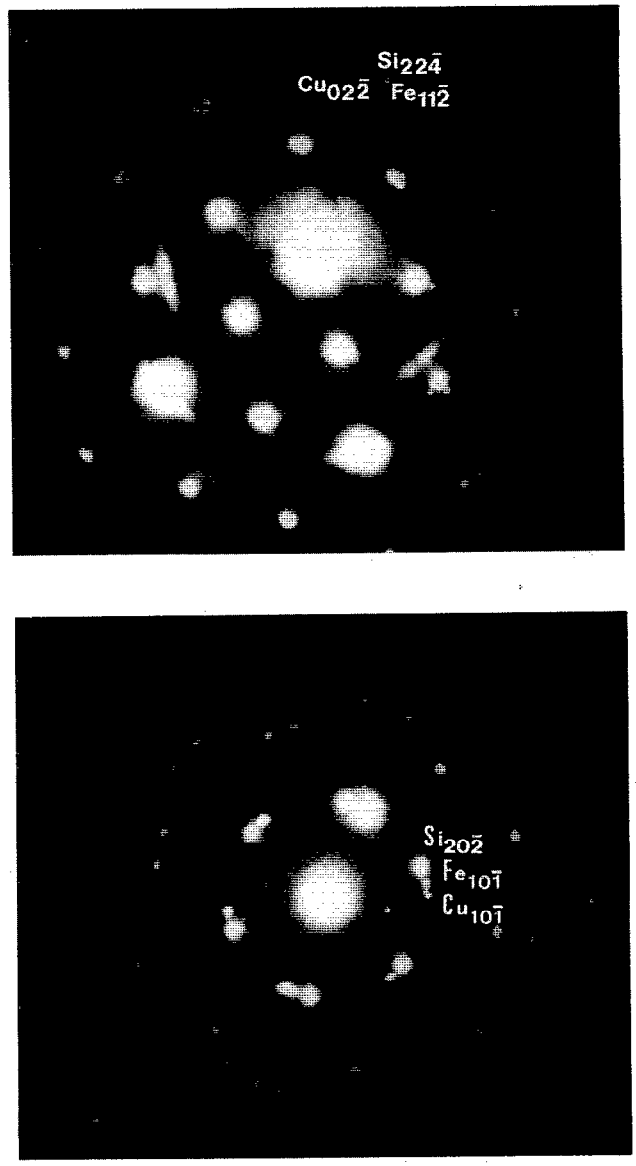

FIG. 5. (a) Electron diffraction pattern of sample 1. Note the satellite spots associated to the hexagonal Si pattern. (b) Electron diffraction pattern of sample 2. Note the rotationally displaced satellite spots relative to the Si pattern. The choice of the metal nearest to Si is crucial for the epitaxial orientation of the superlattices. The Si spots can be indexed and assigned due to the regularity of the hexagonal pattern. The satellite Fe and Cu spots can be indexed using XRD and TEM results, but the assignment is not unambiguous.

DISCUSSION AND CONCLUSIONS

Reviewing the sample preparation conditions mentioned in the Introduction one finds that the vast majority of the epitaxial Fe/Cu bilayers, sandwiches, and multilayers was obtained in ultrahigh vacuum (UHV) and molecular beam epitaxy (MBE) conditions. In contrast we employed experimental deposition conditions far from the stringent MBE constraints and produced epitaxial Fe/Cu superlattices with relative ease on the unreconstructed Si(111) surface. The single most important deposition condition we found for epitaxy at RT is the deposition rate which should be below 1 Å/s for both metals. The vacuum

should be adequate to the chosen rate to prevent significant contamination of the growing film.

The low angle x-ray diffraction results show that these multilayers were indeed deposited as designed. The electron diffraction experiments show that the deposited Fe/Cu multilayers consist of monocrystalline Fe and Cu. Crucial is the choice of the first metal on top of Si(111) for the final crystal orientation of both metals in the superlattice. This fact can also be confirmed with the high angle x-ray diffraction results. The interpretation of the electron diffraction results has to be done in accordance with the high angle x-ray results and is a puzzling task. We present below a proposal for the epitaxial relationships in the two superlattices. Sample 1 which starts with Fe on Si(111) shows a solitary x-ray diffraction peak at $2\theta=44.8°$. We interpret this peak as due to both fcc Cu(111) ($d=2.087$ Å) and bcc Fe(110)($d=2.027$ Å). The Cu lattice should have a 3% compression in the (111) direction to match this peak. Building the superlattice, we start with Fe on Si(111). According to Cheng *et al.*[1] bcc Fe grows on top of Si(111) with the (222) orientation along the normal of the film. The Fe(222) peak does not appear in the x-ray diffractogram. We think that this is due to the fact that this first Fe(222) layer is only 15 Å thick. On this first epitaxial bcc Fe layer with the (222) orientation comes the first fcc Cu layer, which according to the x rays grows in the (111) direction. We can match Cu(022)($d=1.278$ Å) diffraction spots with Si(224)($d=1.108$ Å) as is indicated on Fig. 5(a). Cu(022) is perpendicular to the (111) direction of growth and is of sixfold symmetry matching the Si lattice accordingly. The second Fe layer has to grow, according to the x-ray result, in the (011) direction. We can match Fe(112)($d=1.17$ Å) electron diffraction spots to the Si(224) spots. This is also indicated in Fig. 5(a). Of course the lattice mismatch leads to the decoration of the Si spots. The following bilayers grow according to this description. The second superlattice is more difficult to interpret geometrically. This superlattice starts with Cu on top of Si(111). The x-ray diffractogram shows a peak at $2\theta=137.20$ which can be readily associated with the bcc Fe(222) direction of growth. We have to ask now where is the diffraction signal of Cu in this pattern. We found no meaningful way to associate Cu diffraction to this $2\theta=137.20$ peak nor to any Si(111) peak in this diffractogram. Thus we are forced to assume that Cu has the bcc structure in this second superlattice and adopts the bcc Fe lattice. To understand the construction of the superlattice we start with Cu on top of Si(111). This first Cu layer grows, according to Chang,[2] in the (111) direction with the fcc structure. As with the first sample we find no x-ray diffraction peak for this first thin layer. Walker *et al.*[22] very recently used anomalous x-ray diffraction and explained the Cu epitaxy on Si(111), where both elements have a large misfit in lattice parameters, via a seed layer of a few monolayers of the Cu_3Si silicide. The same mechanism is also described by Neddermeyer.[23] We used RT deposition for our samples and it is hard to understand a silicide formation in this condition. On top of this Cu layer grows bcc Fe(222). We see in the electron diffraction pattern of Fig. 5(b), satellite spots which are rotated angularly relative to the Si spots. Since we assume, based on x-ray diffraction, that the following Cu layers adopt the bcc Fe structure no difficulty is found growing the following bilayers matching bcc Fe to bcc Cu. The angular twist relative to the Si spots can be understood as an in-plane relaxation of the strain between the Fe and Cu layers. Certainly several additional experiments have to be done to completely explain the epitaxy in this last sample.

Thus we develop an explanation on how these superlattices grow geometrically and how it is crucial who the first partner is to the Si substrate. The Mössbauer results indicate that in both superlattices Fe is of the bcc type and ferromagnetic with the magnetic moments in the plane of the substrate. Both superlattices are however strained, as the hyperfine fields follow a distribution and the most probable field is below the 330 kOe bcc Fe bulk value. This finding is in agreement with van Noort *et al.*[13] who also found this reduction in Fe/Cu multilayers, although they grew the multilayers in the (100) direction. A possible explanation is the strain which deforms the original Fe lattice in the superlattice.[24] This would also explain the larger distribution of hyperfine fields in sample 1 where bcc Fe and fcc Cu have to match, while the second superlattice shows less strain because both metals have the same lattice and the strain is relaxed by a relative rotation of both metal lattices.

In conclusion, we find epitaxial Fe/Cu superlattices on Si(111) deposited at RT. The crystalline orientation within the superlattice is dependent on which metal is deposited first on the semiconductor. We are confident that this finding opens several avenues for further fundamental and applied research. We think that in the silicide area, epitaxial metallic superlattices are of special interest. Further epitaxial hybrid ferromagnetic-semiconductor structures like those described by Prinz[25] on GaAs and ZnSe could be used in magnetic device technology directly integrated on silicon. Finally the thriving research on magnetic multilayers could benefit from comparisons of differently crystalline oriented samples to explain the oscillating exchange interactions in those systems.[26]

ACKNOWLEDGMENT

This work was supported by CNPq, a Brazilian research sponsoring agency.

[1] Y. T. Cheng, Y. L. Chen, M. M. Karmarkar, and W. Y. Meng, Appl. Phys. Lett. **59**, 953 (1991).
[2] C. A. Chang, J. Appl. Phys. **67**, 566 (1990).
[3] W. A. Jesser and J. W. Matthews, Philos. Mag. **17**, 595 (1968).
[4] U. Gradmann and P. Tillmanns, Phys. Status. Solidi A **44**, 539 (1977).
[5] W. Kümmerle and U. Gradmann, Phys. Status Solidi A **45**, 171 (1978).
[6] C. Rau, C. Schneider, G. Xing, and K. Jamison, Phys. Rev. Lett. **57**, 3221 (1986).
[7] W. Becker, H. D. Pfannes, and W. Keune, J. Magn. Magn. Mater. **35**, 53 (1983).
[8] R. Halbauer and U. Gonser, J. Magn. Magn. Mater. **35**, 55 (1983).
[9] A. J. Freeman and C. L. Fu, J. Appl. Phys. **61**, 3356 (1987).
[10] B. Heinrich, Z. Celinski, J. F. Cochrane, W. B. Muir, J. Rudd, Q. M.

Zhong, A. S. Arrot, K. Myrtle, and J. Kirschner, Phys. Rev. Lett. **64**, 673 (1990).
[11] Z. Celinski and B. Heinrich, J. Magn. Magn. Mater. **99**, L25 (1991).
[12] F. Ponktees and H. Neddermeyer, Physica B **161**, 276 (1989).
[13] W. R. Bennett, W. Schwarzacher, and W. F. Egelhoff, Jr., Phys. Rev. Lett. **65**, 3169 (1990).
[14] H. M. van Noort, F. J. A. den Broeder, and H. J. G. Draaisma, J. Magn. Magn. Mater. **51**, 273 (1985).
[15] S. S. P. Parkin, R. Bhadra, and K. P. Roche, Phys. Rev. Lett. **66**, 2152 (1991).
[16] F. Petroff, A. Barthélémy, D. H. Mosca, D. K. Lottis, A. Fert, P. A. Schroeder, W. P. Pratt, Jr., R. Loloee, and S. Lequien, Phys. Rev. B **44**, 5355 (1991).
[17] F. Badia, G. Fratucello, B. Martinez, D. Fiorani, A. Labarta, and J. Tejada, J. Magn. Magn. Mater. **93**, 425 (1991).
[18] M. Doyama, M. Matsui, H. Matsuoka, S. Mitani, and K. Doi, J. Magn. Magn. Mater. **93**, 374 (1991).
[19] H. Kiessig, Ann. Phys. **10**, 769 (1931).
[20] C. M. Falco, J. M. Slaughter, and B. N. Engel, Summerschool on Nanostructured Magnetic Materials Crete (1990).
[21] X-ray Powder Diffr. Files JCPDS (Joint Committee on Powder Diffraction Standards, Swarthmore) (1987).
[22] F. J. Walker, E. D. Specht, and R. A. McKee, Phys. Rev. Lett. **67**, 2818 (1991).
[23] H. Neddermeyer, Crit. Rev. Solid State Mater. Sci. **16**, 309 (1990).
[24] J. F. Janak, Phys. Rev. B **20**, 2206 (1979).
[25] G. A. Prinz, Science **250**, 1092 (1990).
[26] R. Coehoorn, Phys. Rev. B **44**, 9331 (1991).